

Biochar as an Effective Alternative to Graphite for Graphene Oxide Synthesis

Martina Fazi^a, Domenico Rosa^a, Francesco Amato^b, Andrea Giacomo Marrani^b, Luca Di Palma^a

^a Department of Chemical Engineering Materials Environment, Sapienza-University of Rome, Via Eudossiana 18, 00184 Rome, Italy

^b Department of Chemistry, Sapienza-University of Rome, Piazzale Aldo Moro 5, 00185 Rome, Italy
martina.fazi@uniroma1.it

This study investigates the preparation of graphene oxide (GO) from biochar as a starting material. GO is a 2D carbon-based nanomaterial used in both its oxidized and reduced forms for applications in electronics, Li-ion batteries, biomedicine, and biosensing. It is produced through exfoliation and oxidation of graphite, which is classified among the European critical raw materials.

In this work, graphite was replaced with biochar, the carbon-rich solid residue produced by biomass pyrolysis. Biochar is highly versatile, with properties that vary depending on its synthesis parameters. In this case, a graphite-like biochar is required, with high carbon content and extended conjugate domains. Slow pyrolysis was selected as a synthesis method. Specifically, considering 900 °C as pyrolysis temperature and licorice roots as biomass, different residence times were employed to investigate their influence on the C sp² content of the product. Biochars prepared in 1 hour, 24 hours, and 48 hours were used for GO synthesis through the Hummers method.

The resulting products were characterized through UV-Visible, Raman, and XPS spectroscopies and a comparison with GO prepared from graphite was performed to assess the suitability of biochar for this application.

1. Introduction

Graphene is one of the carbon allotropes with a honeycomb structure, characterized by exceptional properties such as high thermal and electrical conductivity, transparency, hardness, elasticity, and flexibility (Plenča et al. 2023); indeed, graphene-based materials have been exploited in biomaterial science, optics and electronics, and many other fields of research (Palmieri et al. 2023). Many methods are used to obtain it: one of the most popular methods is top-down mechanical or chemical exfoliation, which allows the separation of graphite into different layers of graphene, overcoming van der Waals forces. Nobel Prize-winning scotch tape method is the most well-known mechanical exfoliation technique, which is simple and effective but not scalable. On the other hand, chemical exfoliation is known for its reliability and suitability for upscaling (Yan et al. 2021a). In general, oxidation of graphite introduces oxygen-containing functional groups, which increase the interlayer spacing between graphene sheets, thereby facilitating their separation. Hummers' method is well-studied to oxidize and exfoliate graphite, producing GO, and its reduction allows to have a product chemically similar to graphene, known as reduced graphene oxide (RGO).

Although graphite is the most common precursor for GO, it is classified as a critical raw material by the EU, Japan, and the United States. As such, identifying alternative, sustainable precursors is of growing importance. A cost-effective and environmentally friendly choice for GO synthesis could be biochar, obtained via pyrolysis of biomass, due to its inherent carbon-rich nature (Plenča et al. 2023). Depending on feedstock biomass and pyrolysis temperature, it is possible to obtain different graphitization degrees. Biochar indeed is characterized by an aromatic structure, which is believed to consist of at least two different aromatic carbon phases: an amorphous phase comprising randomly organized aromatic rings, and a crystalline phase, comprising

condensed polyaromatic sheets that are turbostratically aligned (Wiedemeier et al. 2015). In general, aromatic rings are already visible in biochar at low temperature of pyrolysis (500 °C), but to obtain high aromatic condensation degrees higher temperatures (>1000 °C) are required (Wiedemeier et al. 2015). In fact, that of 1200 °C is usually considered the optimum graphitization temperature for different biomass, like miscanthus (Yan et al. 2021b). However, as highlighted by recent findings, attempts to synthesize graphene-like structures from biochar at temperatures below 1200 °C have so far yielded limited results, with insufficient graphitization degrees for effective GO production (Alhassan et al. 2025).

This study aims to synthesize graphene oxide (GO) at lower temperatures, focusing on how residence time influences the degree of graphitization in biochar. Specifically, licorice roots were used as feedstock biomass, and pyrolyzed at the same temperature of 900 °C for three different residence times: 1, 24, and 48 hours.

To evaluate the feasibility of biochar as an alternative to graphite, the three resulting biochars were used as precursors for GO synthesis via the Hummers method (Mishra et al. 2023). The obtained GO samples were then characterized by UV-Vis, Raman, and XPS spectroscopy, and compared with GO derived from commercial graphite.

2. Materials and methods

2.1 Biochar synthesis

Three samples of biochar were synthesized through slow pyrolysis, starting from agricultural waste. Licorice roots were used as feedstock biomass. They were first washed with water, then dried and finally pressed in an autoclave to obtain an oxygen-limited atmosphere as in a previous work (Rosa et al. 2024). The autoclave was placed in a muffle furnace at 900 °C considering three different residence times (1, 24, and 48 hours). The resulting biochars (BC1, BC24, BC48) were then homogenized using a mortar.

2.2 GO synthesis

The three biochars were used in place of graphite as starting materials to synthesize GO via the Hummers method. In this case, the synthesis procedure described in Amato et al. (2023) was applied to biochar instead of graphite; the workup procedure followed the protocol reported by Amato et al. (2025) and three products were thus obtained, namely GO_BC1, GO_BC24, and GO_BC48.

2.3 Raman spectroscopy

Concentrated solutions of the three products were drop-cast onto Si(100) wafer. The corresponding Raman spectra were collected at room temperature in backscattering geometry, using an inVia Renishaw micro-Raman spectrometer equipped with an air-cooled CCD detector and super-Notch filters. An Ar⁺ ion laser ($\lambda_{\text{laser}} = 514$ nm) was used coupled to a Leica DLML microscope with a 20× objective. The instrument was calibrated using the signal of Si(100) support at 520.5 cm⁻¹, with a spectral resolution of 2 cm⁻¹.

2.4 UV-Visible spectroscopy

Hummers products were analyzed using a Shimadzu UV-2600i Plus spectrophotometer at room temperature, employing quartz cuvettes with a 10 mm path length.

2.5 XPS spectroscopy

50 μ L of an aqueous dispersion of GO_BC48 were drop-cast onto an H-terminated Si(100) wafer. XPS measurements were carried out using an Omicron NanoTechnology Multiprobe MXPS system using a monochromatic Al K α ($h\nu = 1486.7$ eV) X-ray source (Omicron XM-1000, 14 kV and 16 mA) and an analyzer pass energy of 20 eV. A take-off angle of 21° relative to the sample surface normal was adopted. The experimental spectra were curve-fitted using a Shirley function for the secondary electron background and a pseudo-Voigt function (30% Lorentzian weight) for the elastic peaks, with position and full width at half maximum (FWHM) allowed to optimize within narrow limits.

After curve fitting of the C1s region, the content of oxygen can be determined through $R_{O/C}$ ratio (Amato et al. 2025), using the following Equation 1:

$$R_{O/C} = \frac{A_{C-OH} + \frac{1}{2}A_{C-O-C} + A_{C=O} + 2A_{COOH}}{A_{C=C} + A_{C-OH} + A_{C-O-C} + A_{C=O} + A_{COOH}} \quad (1)$$

where A_x is the area of oxygen functional group (OFG) obtained by curve fitting.

The same A_x values can be used to determine the relative amounts of OFGs with an uncertainty of $\pm 10\%$, according to Equation 2 (Amato et al. 2025):

(2)

$$A\%_{OFG} = \frac{A_{C-OH} \text{ or } \frac{1}{2}A_{C-O-C} \text{ or } A_{C=O} \text{ or } A_{COOH}}{A_{C=C} + A_{C-OH} + \frac{1}{2}A_{C-O-C} + A_{C=O} + A_{COOH}} \times 100$$

3. Results and discussion

Below are reported the characterization data of the GO samples: all spectra are compared with literature characterization data of GO obtained from commercial graphite (Amato et al. 2025).

3.1 Raman characterization

Figure 1 shows Raman spectra of the synthesized GO samples. All three spectra exhibit four characteristic peaks located at 1320 cm⁻¹, 1600 cm⁻¹, 2700 cm⁻¹, and 2950 cm⁻¹. The first two peaks correspond to D and G bands, related respectively to the ring breathing mode of sp² carbon rings adjacent to edges or defects, and to the C=C stretching of sp² domains (Amato et al. 2023a). The other two are 2D and D+G bands, which are the second-order signals. In particular, GO_BC1, GO_BC24 and GO_BC48 display I_D/I_G ratios of 0.73, 0.77, and 0.77, respectively.

All spectra are consistent with the Raman spectrum of GO obtained from commercial graphite, which shows the same four bands, located at similar Raman shifts; its I_D/I_G value is 0.87 (Amato et al. 2023a). By comparing the I_D/I_G values, it is evident that with increasing residence time, the defect density in the structure increases, as does the oxidation degree of the Hummers product. However, these values remain lower than that observed in GO obtained from commercial graphite.

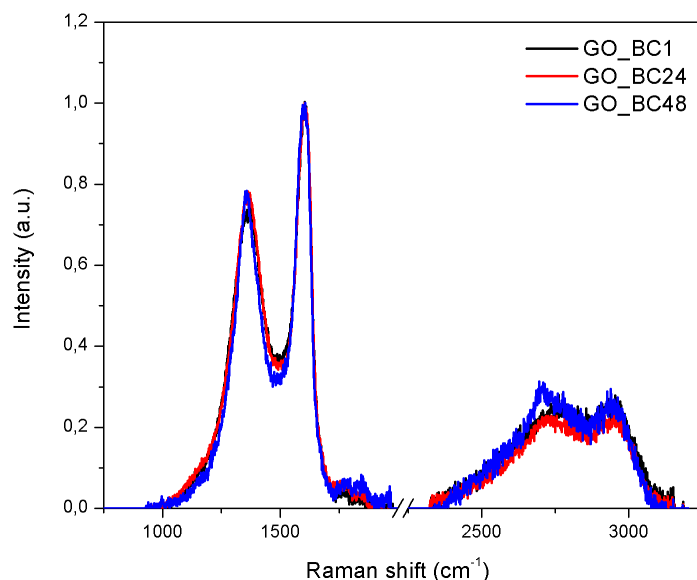


Figure 1: GO_BC1, GO_BC24, and GO_BC48 Raman spectra

3.2 UV-Visible characterization

Figure 2 reports UV-Visible spectra of the Hummers products. All three spectra display two distinctive signals: a peak appearing around 200 nm, which is related to π - π^* transitions of C=C bonds, and a shoulder peak at 275 nm, which is related to n - π^* transitions of C=O bonds. The same signals are also observed in GO from commercial graphite, albeit they appear at different wavelengths, namely at 232 and 300 nm.

The spectral profiles of the three synthesized products show a progressive resemblance to that of GO obtained from commercial graphite as the residence time increases. Considering the λ values in Table 1, a bathochromic shift of the first signal in the spectrum is evident with increasing residence time. This phenomenon can be due to enhanced π -conjugation, which reduces the energy gap between HOMO and LUMO.

Indeed, maintaining the same pyrolysis temperature and increasing residence time, the formation of a structure similar to graphite is thermodynamically favored. Clearly, 48 hours as residence time is not enough to reach the same graphitization degree of commercial graphite, whose peak appears at 232 nm compared to 220 nm in GO_BC48. Concerning the second peak, it is localized at 275 nm for all three GO samples, likely because C=O groups are not involved in conjugation with adjacent π -systems.

Table 1: Characteristic absorption wavelengths in the UV-Vis spectra

Sample	λ (nm)
GO_BC1	202
	275
GO_BC24	205
	275
GO_BC48	220
	275
GO from commercial graphite	232
	300

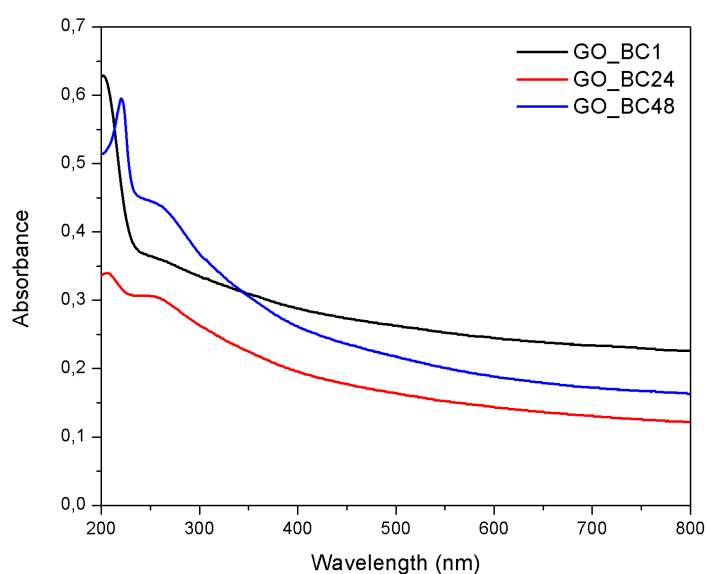


Figure 2: GO_BC1, GO_BC24, and GO_BC48 UV-Visible spectra

3.3 XPS spectra

In Figure 3 the curve-fitted C1s XPS spectrum of GO_BC48 is reported. It displays three main peaks, corresponding to localized sp^2 carbon domains (284.55 eV, red curve), a convolution of C-O bonds from hydroxyl (286.3 eV, blue curve) and epoxide (286.9 eV, green curve), and a convolution of C-O bonds from carbonyl/carboxylate groups (288.1 eV, magenta curve) and carboxyl groups (288.94 eV, dark yellow curve). Considering GO from commercial graphite, a shift in the hydroxyl groups binding energy is observed: it decreases from 286.6 eV (Amato et al. 2025) to 286.3 eV, attributed to their distinct chemical nature. In fact, commercial graphite-based GO contains a higher proportion of basal C-OH groups, while BC_GO48 is richer in phenol-like edges groups (Amato et al. 2023b; Amato et al. 2025).

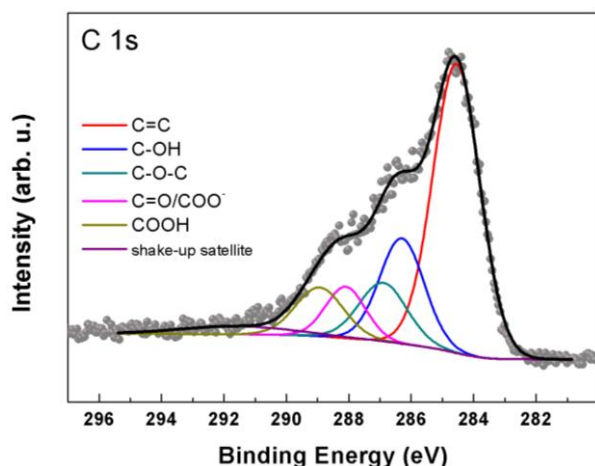


Figure 3: XPS spectrum of GO_BC48

Using Equation 1, an O/C ratio ($R_{O/C}$) of 0.5 was calculated, which is consistent with typical values reported in literature for graphene oxide (Stobinski et al. 2014). This value is higher than that of GO obtained from commercial graphite (see Table 2), indicating a greater oxidation degree in biochar-derived GO.

Using Equation 2, the relative amounts of OFGs were determined; the results are reported in Table 2.

Table 2: $R_{O/C}$ and relative amounts (%) of the OFGs in GO_BC48 and GO from commercial graphite

Sample	$R_{O/C}$	C=C	C-OH	C-O-C	C=O	COOH	Reference
GO_BC48	0.5	56.5	19.5	5.8	8.5	9.7	This work
GO from commercial graphite	0.41	55.8	17.2	18.3	4.1	4.6	(Amato et al. 2025)

According to literature data (Amato et al. 2025), a different distribution of OFGs is observed. Specifically, GO_BC48 shows a higher amount of carbonyl/carboxylate and carboxyl groups, along with a decrease in epoxide groups.

4. Conclusions

In this study, the feasibility of synthesizing GO from biochar was demonstrated, using licorice roots as feedstock biomass in slow pyrolysis process at 900 °C. By varying the residence time, three distinct biochars were obtained and subsequently employed as substitutes for commercial graphite in the Hummers method. Among the resulting GO samples, GO_BC48 (corresponding to a residence time of 48 hours) exhibited the most promising characteristics.

Spectroscopic analyses (UV-Vis, Raman and XPS) revealed a strong similarity between GO_BC48 and commercial graphite GO. Specifically, the sample showed an I_D/I_G ratio of 0.77, indicating a substantial degree of oxidation while maintaining an acceptable level of structural order. UV-Visible spectroscopy revealed a $\pi-\pi^*$ transition of C=C bonds characterized by a bathochromic shift with increasing residence time, consistent with a greater aromatic conjugation and more graphitic structure. XPS analysis revealed an O/C ratio of 0.5, which is higher than that of GO synthesized from commercial graphite, indicating a greater oxidation degree. Additionally, the OFGs distribution revealed a higher content of carbonyl and carboxyl groups, and a lower amount of hydroxyl and epoxide groups.

These features make GO_BC48 a potentially attractive material for various applications. Its high oxidation degree and abundance of acidic functional groups make it particularly suitable for several fields. It can be used in electrochemical devices such as supercapacitors or lithium-ion batteries, where higher oxidation can enhance interactions with aqueous electrolytes and improve electrode wettability. It can be used in composite materials and polymer coatings, where biochar-derived GO can act as a reinforcing or compatibilizing agent due to its good dispersion and chemical reactivity. Additionally, it may be used in biomedical applications such as delivery carriers, due to the presence of reactive groups suitable for further functionalization.

Therefore, biochar proves to be a viable and sustainable alternative to graphite for graphene oxide production, contributing to the valorization of agricultural waste and reducing dependence on critical raw materials.

Nomenclature

BC1 - biochar synthesized from licorice roots pyrolyzed at 900 °C considering 1 hour as residence time.
 BC24 - biochar synthesized from licorice roots pyrolyzed at 900 °C considering 24 hours as residence time.
 BC48 - biochar synthesized from licorice roots pyrolyzed at 900 °C considering 48 hours as residence time.
 GO_BC1 - Hummers product using BC1 as starting material.
 GO_BC24 - Hummers product using BC24 as starting material.
 GO_BC48 - Hummers product using BC48 as starting material.

References

- Alhassan, H., Yoong, V.N., Soon, Y.W., Usman, A., Bakar, M.S.A., Ahmed, A. and Luengchavanon, M. 2025. The differential influence of biochar and graphite precursors on the structural, optical, and electrochemical properties of graphene oxide. *Materials Chemistry and Physics* 329. doi: 10.1016/j.matchemphys.2024.130070.
- Amato, F., Perini, G., Friggeri, G., Augello, A., Motta, A., Giaccari, L., Zanoni, R., De Spirito, M., Palmieri, V., Marrani, A.G. and Papi, M. 2023a. Unlocking the Stability of Reduced Graphene Oxide Nanosheets in Biological Media via Use of Sodium Ascorbate. *Advanced Materials Interfaces* 10(22). doi: 10.1002/admi.202300105.
- Amato, F., Fazi, M., Giaccari, L., Colecchia, S., Perini, G., Palmieri, V., Papi, M., Altimari, P., Motta, A., Giustini, M., Zanoni, R. and Marrani, A.G. 2025. Isolation by dialysis and characterization of luminescent oxidized carbon nanoparticles from graphene oxide dispersions: a facile novel route towards a more controlled and homogeneous substrate with a wider applicability *. *Nanotechnology* 36(18), p. 185602. Available at: <https://iopscience.iop.org/article/10.1088/1361-6528/adc608>.
- Amato, F., Ferrari, I., Motta, A., Zanoni, R., Dalchiele, E.A. and Marrani, A.G. 2023b. Assessing the evolution of oxygenated functional groups on the graphene oxide surface upon mild thermal annealing in water. *RSC Advances* 13(42), pp. 29308–29315. doi: 10.1039/d3ra05083a.
- Amato, F., Motta, A., Giaccari, L., Di Pasquale, R., Scaramuzza, F.A., Zanoni, R. and Marrani, A.G. 2023c. One-pot carboxyl enrichment fosters water-dispersibility of reduced graphene oxide: a combined experimental and theoretical assessment. *Nanoscale Advances* 5(3), pp. 893–906. doi: 10.1039/d2na00771a.
- Mishra, R., Kumar, A., Singh, E., Kumari, A. and Kumar, S. 2023. Synthesis of graphene oxide from biomass waste: Characterization and volatile organic compounds removal. *Process Safety and Environmental Protection* 180, pp. 800–807. doi: 10.1016/j.psep.2023.10.048.
- Palmieri, V., Amato, F., Marrani, A.G., Friggeri, G., Perini, G., Augello, A., De Spirito, M. and Papi, M. 2023. Graphene oxide-mediated copper reduction allows comparative evaluation of oxygenated reactive residues exposure on the materials surface in a simple one-step method. *Applied Surface Science* 615. doi: 10.1016/j.apsusc.2022.156315.
- Plenča, K., Cvetnić, S., Prskalo, H., Kovačić, M., Cvetnić, M., Kušić, H., Matusinović, Z., Kraljić Roković, M., Genorio, B., Lavrenčić Štanger, U. and Lončarić Božić, A. 2023. Biomass Pyrolysis-Derived Biochar: A Versatile Precursor for Graphene Synthesis. *Materials* 16(24). doi: 10.3390/ma16247658.
- Rosa, D., Petruccelli, V., Iacobi, M.C., Brasili, E., Badiali, C., Pasqua, G. and Di Palma, L. 2024. Functionalized biochar from waste as a slow-release nutrient source: Application on tomato plants. *Heliyon* 10(8). doi: 10.1016/j.heliyon.2024.e29455.
- Stobinski, L., Lesiak, B., Malolepszy, A., Mazurkiewicz, M., Mierzwa, B., Zemek, J., Jiricek, P. and Bieloshapka, I. 2014. Graphene oxide and reduced graphene oxide studied by the XRD, TEM and electron spectroscopy methods. *Journal of Electron Spectroscopy and Related Phenomena* 195, pp. 145–154. doi: 10.1016/j.elspec.2014.07.003.
- Wiedemeier, D.B., Abiven, S., Hockaday, W.C., Keiluweit, M., Kleber, M., Masiello, C.A., McBeath, A.V., Nico, P.S., Pyle, L.A., Schneider, M.P.W., Smernik, R.J., Wiesenberger, G.L.B. and Schmidt, M.W.I. 2015. Aromaticity and degree of aromatic condensation of char. *Organic Geochemistry* 78, pp. 135–143. doi: 10.1016/j.orggeochem.2014.10.002.
- Yan, Y., Manickam, S., Lester, E., Wu, T. and Pang, C.H. 2021a. Synthesis of graphene oxide and graphene quantum dots from miscanthus via ultrasound-assisted mechano-chemical cracking method. *Ultrasonics Sonochemistry* 73. doi: 10.1016/j.ultsonch.2021.105519.
- Yan, Y., Meng, Y., Zhao, H., Lester, E., Wu, T. and Pang, C.H. 2021b. Miscanthus as a carbon precursor for graphene oxide: A possibility influenced by pyrolysis temperature. *Bioresource Technology* 331. doi: 10.1016/j.biortech.2021.124934.